Supplementary Information

Efficient near-infrared emission from lead-free ytterbium-doped cesium bismuth halide perovskites

Minh N. Tran, Iver J. Cleveland, Gregory A. Pustorino, and Eray S. Aydil*

Department of Chemical and Biomolecular Engineering, Tandon School of Engineering, New York University, 6 Metrotech Center, Brooklyn, NY 11201, United States

* e-mail: aydil@nyu.edu

Near-Infrared Photoluminescence Quantum Yield Calculation

Photoluminescence (PL) spectra were excited and detected using a QuantaMaster-8075-21 (Horiba) spectrophotometer. Near-infrared PL was excited at 360 nm and 420 nm for ytterbium-doped cesium bismuth bromide ($Cs_3Bi_2Br_9$) and mixed halide ($Cs_3Bi_2(Br_{1-y}I_y)_9$) films, respectively. A photomultiplier tube was used to measure visible excitation light, and NIR PL was detected using liquid nitrogen cooled InGaAs detector. PLQY was measured using an integrating sphere (Quanta-Phi, Horiba), and the lamp power was measured using Power Meter 843-R and 818-UV photodetector (both Newport). The two detectors were calibrated to convert their signals to the number of photons/s. A power meter was used to measure the Xenon lamp power at the emission and excitation peak (5 nm bandwidth). The calibration constant for each detector is calculated from

$$X_{cal} = \frac{Number\ of\ photons\ detected\ by\ the\ power\ meter}{Integrated\ detector\ signal} = \frac{\frac{P}{\left(\frac{hc}{\lambda}\right)}}{\int I_{cal} d\lambda}$$

where X_{cal} is the calibration constant, P is the total Xe lamp power in 5 nm bandwidth at λ, h is Planck's constant, c is the speed of light. λ is the excitation peak wavelength or the emission peak wavelength for calibration of the PMT detector or the InGaAs detector, respectively. I_{cal} is the detector signal as the detection monochromator is scanned across the excitation or the emission wavelength. The denominator is this signal integrated across a bandwidth of 5 nm.

Photoluminescence quantum yield (PLQY) is then calculated using

$$PLQY = \frac{\int_{\lambda_{em}} [I_s(\lambda) - I_{ref}(\lambda)] d\lambda}{\int_{\lambda_{ex}} [I_{ref}(\lambda) - I_s(\lambda)] d\lambda} \times \frac{X_{cal,em}}{X_{cal,ex}} \times 100\ \%$$

where λ_{em} and λ_{ex} are the emission and the excitation wavelengths, respectively, $I_s(\lambda)$ and $I_{ref}(\lambda)$ are the detector signal from the sample and a glass reference, respectively. The integrals are across the emission and excitation peaks as denoted beneath the integrals. $X_{cal,em}$ and $X_{cal,ex}$ are the calibration constants for the InGaAs detector (used for NIR emission) and PMT detector (used for UV and visible excitation), respectively.

Also, the PMT detector was calibrated independently using Rhodamine 6G dye (99%, Acros Organics) and yielded a PLQY of 89.4% (literature value is 89-92%).[1,2] InGaAs detector was calibrated independently using IR 140 dye (95%, Aldrich), and the above procedure yielded a PLQY of 18.0% (literature value 16.7-20%).[3,4] IR140 dye was excited at 765 nm so that the excitation light could be measured using both the PMT and the InGaAs detector. The calculated PLQY using two detectors is 18.0%, close to the PLQY calculated using only the InGaAs detector (18.6%).

Comparison of UV-Visible PL from the literature attributed to $Cs_3Bi_2Br_9$ Nanocrystals with UV-Visible PL from $BiBr_3$ and OA solutions in various solvents

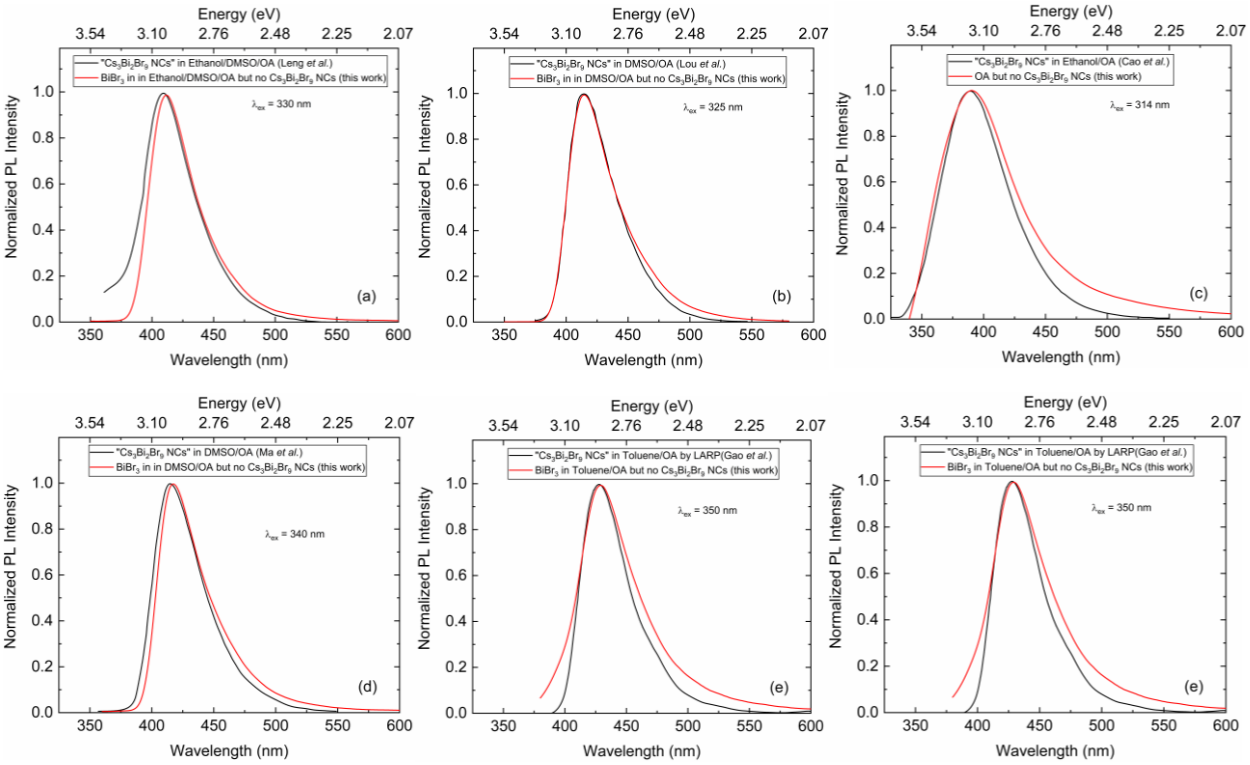

Figure S1. Comparison of normalized PL intensities assigned to $Cs_3Bi_2Br_9$ nanocrystals (NCs) from various publications and PL from $BiBr_3$ and oleic acid (OA) in different solvents used in those publications. The PL data are extracted from plots published in the respective references via digitization using WebPlotDigitizer and then normalized to the highest value. The PL measured in this work is also normalized to the highest value. The solutions are prepared as described in the main text. The PL was excited at the same wavelength, λ_{ex}, as the referenced work if they reported the excitation wavelength or the peak wavelength of their excitation scan. (a) PL from Leng *et al.*,[5] assigned to $Cs_3Bi_2Br_9$ NCs compared to PL from $BiBr_3$ in ethanol, dimethyl sulfoxide (DMSO), and OA. (b) PL from Lou *et al.*[6] assigned to $Cs_3Bi_2Br_9$ NCs compared to PL from $BiBr_3$ in DMSO and OA. (c) PL from Cao *et al.*[7] assigned to $Cs_3Bi_2Br_9$ NCs compared to PL from OA. (d) PL from Ma *et al.*[8] assigned to $Cs_3Bi_2Br_9$ NCs compared to PL from $BiBr_3$ in DMSO and OA. (e) PL from Gao *et al.*[9] assigned to $Cs_3Bi_2Br_9$ NCs synthesized by the LARP method compared to PL from $BiBr_3$ in OA and Toluene. (f) PL from Lian *et al.*[10] assigned to $Cs_3Bi_2Br_9$ NCs compared to PL from $BiBr_3$ in OA and Hexane.

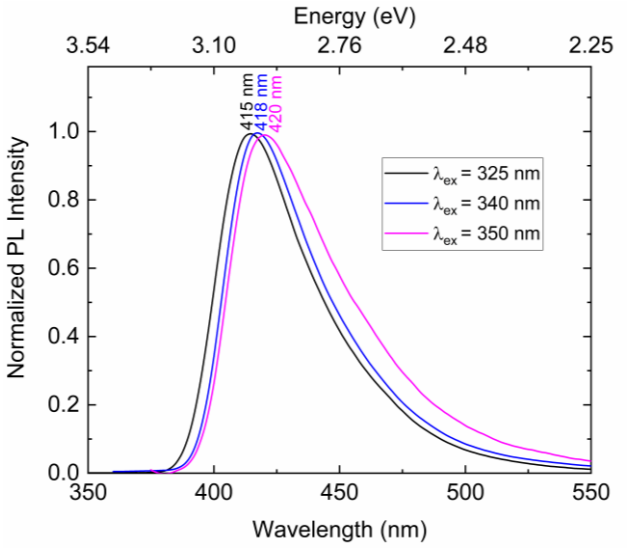

Figure S2. Photoluminescence from $BiBr_3$ in DMSO and OA when excited at different wavelengths, λ_{ex}.

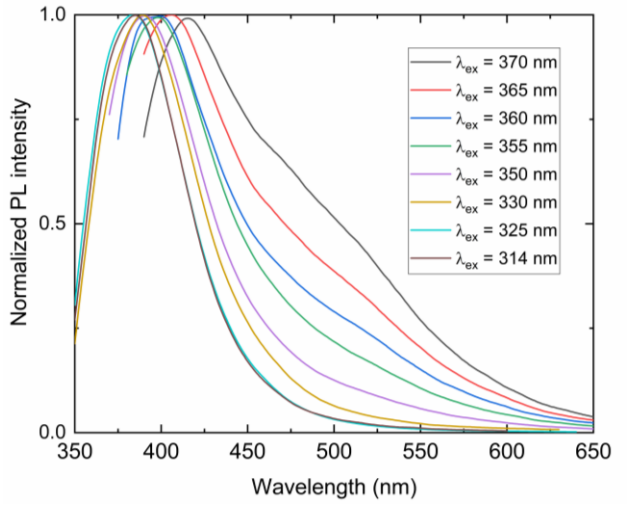

Figure S3. PL from commercial oleic acid (90%, Alfa Aesar) when excited at different wavelengths, λ_{ex}.

Table S1. Reported PL from $Cs_3Bi_2Br_9$ nanocrystals and their corresponding sizes from literature.

$Cs_3Bi_2Br_9$ nanocrystal size	**Reported PL peaks**	**Reference**
3.3 nm	446 nm	Ding *et al.*[11]
3.5 nm	414 nm	Lou *et al.*[6]
3.88±0.67 nm	410 nm	Leng *et al.*[5]
4.80±1.24 nm	389 nm	Cao *et al.*[7]
6±2 nm	468 nm	Yang *et al.*[12]
10.44±1.29 nm	414 and 433 nm	Gao *et al.*[9]
15 nm	427 and 460 nm	Nelson *et al.*[13]
9 nm thickness, 60-250 nm length	427 nm	Lian *et al.*[10]
Nanocomposites with BiOBr	414 nm	Ma *et al.*[8]

Table S2. The Yb concentration in each film is reported as the atomic ratio of [Yb]/[Bi] calculated from QCM rates, the atomic percentage calculated from QCM rates, and the atomic percentage calculated from the EDS measurements. The EDS peaks of Yb and Br overlap ($L\alpha_{Br}$ = 1.48 keV, $M\alpha_{Yb}$ = 1.52 keV.)

The atomic ratio from the QCM rates (%) $\frac{[Yb]}{[Bi]}$	At. % of Yb^{3+} from to QCM rates (%) $\frac{[Yb]}{[Cs]+[Bi]+[Yb]+[Br]}$	At. % of Yb^{3+} from EDS (%) $\frac{[Yb]}{[Cs]+[Bi]+[Yb]+[Br]}$
10	1.4	0.7
15	2.0	1.2
20	2.6	1.6
30	3.7	2.0
40	4.8	2.3
50	5.7	3.0

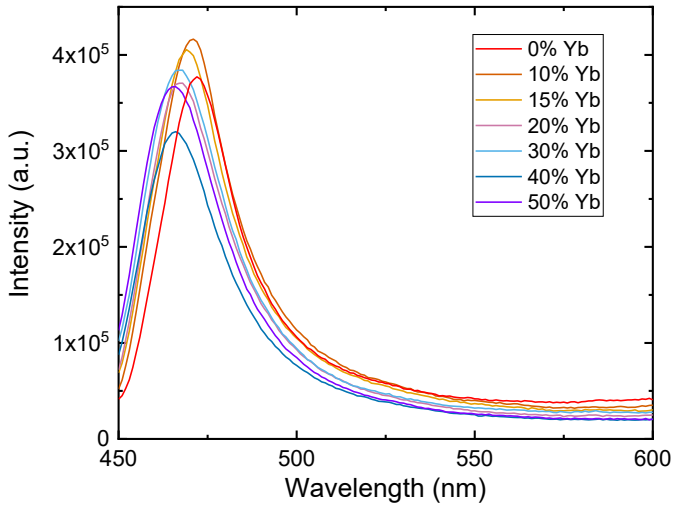

Figure S4. Raw visible emissions of undoped and Yb-doped $Cs_3Bi_2Br_9$ films.

REFERENCES

1. C. Würth, M. G. González, R. Niessner, U. Panne, C. Haisch and U. Resch-Genger. *Talanta*, 2012, **90**, 30-37.
2. C. Würth, M. Grabolle, J. Pauli, M. Spieles and U. Resch-Genger. *Anal. Chem.*, 2011, **83**, 3431-3439.
3. K. Rurack and M. Spieles. *Anal. Chem*., 2011, **83**, 1232-1242.
4. S. Hatami, C. Würth, M. Kaiser, S. Leubner, S. Gabriel, L. Bahrig, V. Lesnyak, J. Pauli, N. Gaponik, A. Eychmüller and U. Resch-Genger. *Nanoscale*, 2015, **7**, 133-143.
5. M. Leng, Y. Yang, K. Zeng, Z. Chen, Z. Tan, S. Li, J. Li, B. Xu, D. Li, M. P. Hautzinger, Y. Fu, T. Zhai, L. Xu, G. Niu, S. Jin and J. Tang. *Adv. Funct. Mater.,* 2018, **28**, 1704446.
6. Y. Lou, M. Fang, J. Chen and Y. Zhao. *Chem. Commun.*, 2018, **54**, 3779-3782

7. Y. Cao, Z. Zhang, L. Li, J. Zhang and J. Zhu. *Anal. Chem*., 2019, **91**, 8607-8614.
8. Z. Ma, Z. Shi, L. Wang, F. Zhang, D. Wu, D. Yang, X. Chen, Y. Zhang, C. Shan and Z. Li. *Nanoscale*, 2020, **12**, 3637-3645.
9. M. Gao, C. Zhang, L. Lian, J. Guo, Y. Xia, F. Pan, X. Su, J. Zhang, H. Li and D. Zhang. *J. Mater. Chem. C.*, 2019, **7**, 3688-3695.
10. L. Lian, G. Zhai, F. Cheng, Y. Xia, M. Zheng, J. Ke, M. Gao, H. Liu, D. Zhang, L. Li, J. Gao, J. Tang and J. Zhang. *CrystEngComm*, 2018, **20**, 7473-7478.
11. N. Ding, D. Zhou, G. Pan, W. Xu, X. Chen, D. Li, X. Zhang, J. Zhu, Y. Ji and H. Song. *ACS Sustain. Chem. Eng.,* 2019, **7**, 8397-8404.
12. B. Yang, J. Chen, F. Hong, X. Mao, K. Zheng, S. Yang, Y. Li, T. Pullerits, W. Deng and K. Han. *Angew. Chem. Int. Ed*., 2017, **56**, 12471-12475.
13. R. D. Nelson, K. Santra, K.; Y. Wang, A. Hadi, J.W. Petrich and M. G. Panthani, M.G. *Chem. Commun*., 2018, **54**, 3640-3643.